PHYSICAL REVIEW D VOLUME 43, NUMBER 3 1 FEBRUARY 1991

Intermediate-mass Higgs boson at hadron supercolliders

V. Barger, G. Bhattacharya, T. Han,* and B. A. Kniehl
Physics Department, University of Wisconsin, Madison, Wisconsin 53706
(Received 20 August 1990)

We study the inclusive production at future hadron supercolliders of the standard-model Higgs boson in the intermediate-mass region ($M_W \lesssim M_H \lesssim 2M_Z$) and its subsequent decay into two virtual W bosons that decay leptonically. Backgrounds from continuum W pair production and from top-quark pair production with semileptonic decays are investigated. We conclude that the Higgs-boson signal may be observed via the decay $H \to W^* W^* \to (l\bar{\nu}_l)(\bar{l}'\nu_{l'})$ at the Superconducting Super Collider for 145 GeV $< M_H \lesssim 2M_Z$ if $m_t > 150$ GeV. Here W^* denotes an on- or off-shell W boson.

I. INTRODUCTION

The understanding of the electroweak symmetry-breaking mechanism (EWSB) in the phenomenologically successful minimal standard model (SM) is currently one of the central problems in particle physics. A single neutral scalar particle, the Higgs boson, remains in the physical spectrum after the EWSB and provides the most direct experimental access to this crucial aspect of the model. The experimental discovery of the Higgs boson is thus among the most challenging goals at present and future accelerators. Although its interactions with other particles are fixed, the theory does not specify the mass of the Higgs boson, M_H, which renders direct experimental Higgs-boson searches difficult.[1,2] The experimental lower bound $M_H > 41.6$ GeV has recently been obtained[3] at the CERN Large Electron Positron Collider (LEP). On the other hand, if M_H exceeds 1 TeV, the Higgs boson interacts strongly with the W and Z bosons, and its particle properties disappear.[4]

At the Z factories, LEP I and the SLAC Linear Collider (SLC), it will be possible to search for the SM Higgs bosons with mass $M_H \lesssim M_Z/2$ via the Bjorken process[5] $e^+e^- \to Z \to Hf\bar{f}$. At LEP II, with $\sqrt{s} = 200$ GeV, the Higgs-boson search can be continued using the bremsstrahlung process $e^+e^- \to Z^* \to ZH$, the Higgs-boson discovery limit being then[1,6] $M_H \lesssim M_W$. Heavier Higgs bosons require accordingly higher values of $\sqrt{s}$. However, the cross section for the above-mentioned process falls off as $1/s$ as s increases. Fortunately, the cross section for the WW fusion process,[7] $e^+e^- \to \nu\bar{\nu}WW \to \nu\bar{\nu}H$, grows as $\log(s/M_W^2)$ and becomes dominant over the bremsstrahlung process for $\sqrt{s} \gtrsim 0.3$ TeV $+ M_H$. In general,[1] it should be possible to observe Higgs-boson signals with $M_H \lesssim \sqrt{s}/2$.

However, an e^+e^- collider with an energy exceeding that of LEP II will not be available in the foreseeable future. Thus the next generation of hadron colliders, such as the Superconducting Super Collider (SSC) and the CERN Large Hadron Collider (LHC), will serve as the main tools to discover the Higgs boson. The high-mass Higgs boson ($2M_Z < M_H < 1$ TeV) should be found at these hadron colliders.[1,2] However, searches for the intermediate-mass Higgs boson (IMH), defined by $M_W \lesssim M_H \lesssim 2M_Z$, face severe problems. Although the IMH can be copiously produced at future multi-TeV pp colliders, the signals for the IMH are either obscured by substantial backgrounds or have low rates after choosing clean triggers.[1,8] Both production and decay of the IMH will depend upon the top-quark mass. Current experimental searches for the top quark suggest[9] $m_t > M_W$. Thus the decay mode $H \to t\bar{t}$ is kinematically forbidden for the IMH and $H \to b\bar{b}$ will be dominant; as a consequence, the leptonic and other rare decay modes of the Higgs boson attain relative importance. In addition, QCD corrections[10] tend to decrease the partial widths for hadronic Higgs-boson decays, which gives rise to a relative enhancement of the branching fractions into leptonic and other rare decay channels.

Continuum $b\bar{b}$ production overwhelms the $H \to b\bar{b}$ signal. The main leptonic channel $H \to \tau^+\tau^-$ is of limited use only: In the dominant single-charged-particle decays of the τ leptons, the missing momentum carried by neutrinos introduces an uncertainty in the $\tau^+\tau^-$ invariant mass;[11] also, the observation of two τ's from their hadronic decay products is problematic in the environment of a hadron collider unless vertex detectors can be used. As for the mode $H \to \gamma\gamma$, even with an excellent photon energy resolution of 1%, it appeared to be extremely difficult to discern the signal from the continuum background;[12] however, it has been recently claimed[13] that the proposed L^* SSC detector achieves the necessary background rejection to see the $H \to \gamma\gamma$ signal by photon isolation criteria. The mode[8] $H \to Z\gamma$ is likely to be more difficult to distinguish from backgrounds than $H \to \gamma\gamma$.

One of the most promising IMH decay modes is that into one real and one virtual weak vector boson.[14] It has been shown[15] that this signal is dominated by SM backgrounds if at least one of the vector bosons decays hadronically. Subsequent works[8,16] have thus focused on leptonic decays of both vector bosons.

It has been claimed[17] recently that the "gold-plated" mode $H \to ZZ^* \to (l\bar{l})(l'\bar{l}')$ may be useful for IMH searches with a suitably designed detector in spite of relatively small rates and severe backgrounds such as $b\bar{b}b\bar{b}$.

In this paper we focus attention on an inclusively pro-

duced IMH that decays through two virtual W bosons into $(l\bar{\nu}_l)(\bar{l}'\nu_{l'})$. The branching fractions of the corresponding modes for Z bosons are smaller by about one order of magnitude. We analyze possible background processes at SSC and LHC, including that from top-quark pair production with semileptonic decays, which has become relevant due to the new Collider Detector at Fermilab (CDF) lower limit[9] on m_t and has not been considered in this context before. The most severe backgrounds are due to continuum WW and $t\bar{t}$ production.

The organization of this paper is as follows: In Sec. II we calculate the branching fractions for the IMH decays into W^*W^* and Z^*Z^*. In Sec. III we compare the signal for $H\to W^*W^*$ with the various background processes. Our conclusions are summarized in Sec. IV.

II. BRANCHING FRACTIONS FOR HIGGS-BOSON DECAY INTO TWO VIRTUAL VECTOR BOSONS

Figure 1 shows the Feynman diagram for the decay of a Higgs boson into two vector bosons V_1 and V_2, which on their part decay into nonidentical fermion pairs:

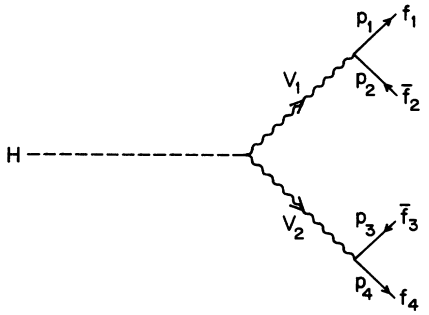

FIG. 1. Feynman diagram for decay of the Higgs boson into two virtual vector bosons.

$$H\to V_1V_2\to(f_1\bar{f}_2)(\bar{f}_3f_4)\ . \tag{1}$$

In the massless-fermion approximation, the differential decay rate is given by

$$d\Gamma=\frac{C_V^2}{M_H}(G_1p_1\cdot p_4p_2\cdot p_3+G_2p_1\cdot p_3p_2\cdot p_4)|D_{V_1}(p_{V_1})|^2|D_{V_2}(p_{V_2})|^2dP_4(p_H;p_1,\ldots,p_4)\ , \tag{2}$$

where $D_V(p)=(p^2-M_V^2+iM_V\Gamma_V)^{-1}$ is the denominator of the vector-boson propagator, and the n-body phase-space element is given by

$$dP_n(p;p_1,\ldots,p_n)=(2\pi)^4\delta^4\left[p-\sum_{i=1}^n p_i\right]\prod_{i=1}^n\frac{d^3p_i}{(2\pi)^3 2E_i}\ . \tag{3}$$

The constant C_V represents the HV_1V_2 coupling and

$$G_1=(g_{1L})^2(g_{2L})^2+(g_{1R})^2(g_{2R})^2\ , \tag{4}$$

$$G_2=(g_{1L})^2(g_{2R})^2+(g_{2L})^2(g_{1R})^2\ , \tag{5}$$

with

$$g_{iL,R}=g_{iV}\mp g_{iA}\quad(i=1,2)\ . \tag{6}$$

Here g_{iV} and g_{iA} are the vector and axial-vector couplings, respectively, of the fermionic decay currents to V_i. Equation (2) incorporates the full matrix element for the decay (1) and is valid for vector bosons both on and off mass shell. We are concerned here with the following two special cases:

$$\text{case I:}\quad V_1=W^{-*},\quad V_2=W^{+*};\quad f_1=l,\quad \bar{f}_2=\bar{\nu}_l,\quad \bar{f}_3=\bar{l}',\quad f_4=\nu_{l'}\ , \tag{7}$$

$$\text{case II:}\quad V_1=Z^*,\quad V_2=Z^*;\quad f_1=l,\quad \bar{f}_2=\bar{l},\quad \bar{f}_3=\bar{\nu}_{l'},\quad f_4=\nu_{l'}\ . \tag{8}$$

In order to obtain the total decay rate Γ, one needs to integrate over the phase space accessible to the final-state fermions. It is convenient to decompose this four-body phase space into three two-body phase spaces and to introduce the variables

$$\theta_i=\arctan\left[\frac{M_{V_i}^2-M_V^2}{M_V\Gamma_V}\right]\quad(i=1,2)\ , \tag{9}$$

where the squares of the invariant masses of the virtual vector bosons, $M_{V_i}^2=p_{V_i}^2$, are constrained by $M_{V_1}+M_{V_2}\le M_H$, and M_V,Γ_V denote the mass and width of the corresponding real vector boson. The differential decay rate is then given by

$$d\Gamma=\frac{C_V^2}{M_H}\frac{G_1p_1\cdot p_4p_2\cdot p_3+G_2p_1\cdot p_3p_2\cdot p_4}{M_V^2\Gamma_V^2}\times\prod_{i=1}^2 d\theta_i dP_2(p_H;p_{V_1},p_{V_2})dP_2(p_{V_1};p_1,p_2)\times dP_2(p_{V_2};p_3,p_4)\ . \tag{10}$$

With $x_W=\sin^2\theta_W$ and $g^2=4\pi\alpha/x_W$, the parameters in Eq. (10) for the two cases are

case I: $M_V=M_W$, $C_V^2=8g^6M_W^2$,

$$g_{iV}=-g_{iA}=\frac{1}{2\sqrt{2}} \quad (i=1,2) ; \tag{11}$$

case II: $M_V=M_Z$, $C_V^2=8g^6M_Z^2/(1-x_W)^3$,

$$g_{1V}=-\tfrac{1}{4}+x_W, \quad g_{1A}=\tfrac{1}{4} ,$$

$$g_{2V}=-g_{2A}=\tfrac{1}{4} . \tag{12}$$

The eight-dimensional integration is performed using Monte Carlo methods. In all our calculations we assume the following values for the vector-boson masses suggested by recent collider runs:[18]

$$M_W=80.0 \text{ GeV}, \quad M_Z=91.17 \text{ GeV} .$$

In case I we sum over the four lepton combinations from $l,l'=e,\mu$ and in case II over the six combinations from $l=e,\mu$ and $\nu_{l'}=\nu_e,\nu_\mu,\nu_\tau$.

To calculate the total Higgs-boson width Γ_H, we have taken into account the tree-level decays into $f\bar{f}$, W^*W^*, and Z^*Z^*, as well as the loop-induced decays into gg, $\gamma\gamma$, and $Z^*\gamma$. Among the loop-induced decays, only $H\to gg$ is appreciably sensitive to m_t; however, the m_t dependence is feeble for $m_t>90$ GeV. We have included the QCD radiative corrections[10] to $H\to q\bar{q}$ using the representation of α_s in the modified minimal-subtraction ($\overline{\text{MS}}$) scheme[19] and using the value $\Lambda_{\overline{\text{MS}}}^{(4)}=0.2$ GeV. In terms of the tree-level partial decay width $\Gamma_0(H\to q\bar{q})$, the radiatively corrected width is

$$\Gamma(H\to q\bar{q})=\Gamma_0(H\to q\bar{q})\left[\frac{\alpha_s(m_H)}{\alpha_s(2m_q)}\right]^{24/(33-2N_f)} \times\left[1+3\frac{\alpha_s(m_H)}{\pi}\right] , \tag{13}$$

where N_f is the number of active quark flavors at scale m_H.

The QCD corrections significantly suppress the tree-level decay rates, in particular by about 30% for the dominant mode $H\to b\bar{b}$ at $M_H=140$ GeV, and thus considerably enhance the branching fractions of interest.

If the mass-shell condition is imposed on the Z boson, the decay mode $H\to Z\gamma$ becomes phase-space suppressed for $M_H\gtrsim M_Z$. For the sake of consistency, we therefore consider $H\to Z^*\gamma\to(l\bar{l}+\nu\bar{\nu})\gamma$. To that end, we convolute the squared matrix element appropriate for the off-shell situation[20] with a Breit-Wigner distribution similarly as in Ref. 21. Analogously to the context of the crossed process $e^+e^-\to H\gamma$, which has been discussed in detail in Ref. 20, there are additional diagrams for $H\to l\bar{l}\gamma$ which, strictly speaking, are necessary to maintain gauge invariance with respect to the photon. However, because of the absence of the s-channel pole from the Z propagator, these diagrams are greatly suppressed for $M_H\lesssim M_Z$ in the gauge used. (On Z resonance a relative suppression factor of $\frac{1}{500}$ has been found in Ref. 20.) For $M_H>M_Z$ our Breit-Wigner approach smoothly matches with the on-shell Z result.

The resulting branching fractions are displayed in Fig. 2 with a choice of $m_t=200$ GeV. For $M_H\lesssim 120$ GeV, $H\to\tau^+\tau^-$ is the dominant leptonic decay mode. But for higher values of M_H the mode $H\to W^*W^*\to(l\bar{\nu}_l)(\bar{l}'\nu_{l'})$ assumes this role. Except for the W^*W^* mode, all branching fractions exhibit a sharp downward dip around the threshold $M_H=2M_W$. This is due to the fact that the partial width for $H\to W^*W^*$ becomes very large near the threshold compared to those for other modes, and it dramatically increases Γ_H. As a consequence, the branching fraction $B(H\to Z^*Z^*)$ assumes a relative maximum at $M_H\approx 150$ GeV. We also see that $B(H\to Z^*\gamma\to(l\bar{l}+\nu\bar{\nu})\gamma)$ is smaller than $B(H\to Z^*Z^*\to l\bar{l}\nu\bar{\nu})$. For comparison we also show the corresponding results for Higgs-boson decay into one real and one virtual vector boson (W^*W, Z^*Z), as well as into $Z\gamma$ (see dotted curves). As has been pointed out in Ref. 21, the analytic expressions for $\Gamma(H\to V^*V)$ ($V=W,Z$) as derived in Ref. 14 are valid in the intermediate-mass region only: They vanish for $M_H<M_V$ and essentially lead to double counting for $M_H>2M_V$. In contrast, Eq. (2) is valid for all values of M_H. The total decay width of the IMH is very narrow; Γ_H is less than 0.5% of M_H.

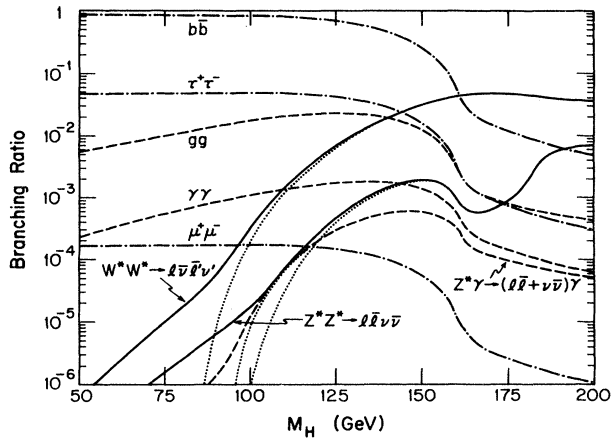

FIG. 2. Branching ratios for the decay of the intermediate-mass Higgs boson. The dotted curves represent the branching ratios for $H\to W^*W$, Z^*Z, and $Z\gamma$.

III. INCLUSIVE PRODUCTION OF HIGGS BOSON IN pp COLLISIONS AND ITS DECAY INTO TWO VIRTUAL W BOSONS

The principal mechanism for the inclusive production of an IMH at hadron supercolliders is through gluon fusion, which proceeds via quark triangle diagrams.[22] The dominant contribution comes from the virtual top quark, and hence the production cross section is mostly sensitive to m_t. In Fig. 3 we show the production cross sections at the SSC and LHC energies versus M_H for selected values of m_t. At SSC energies [Fig. 3(a)] the cross section is generally of the order of 50 pb. For $M_H<100$ GeV the cross section does not depend much on m_t, while for larger M_H it decreases slightly as m_t increases. The cross sections at the LHC [Fig. 3(b)] are approximately 3–4 times smaller than those at the SSC.

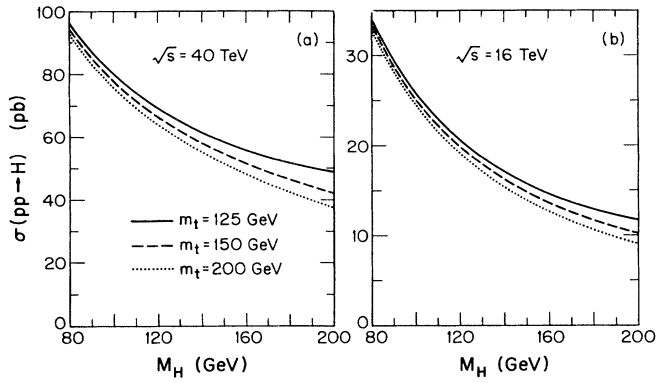

FIG. 3. Production cross sections for the intermediate-mass Higgs boson at the SSC and LHC shown for different values of the top-quark masses.

This is mainly due to the strong decrease of the gluon luminosity at lower center-of-mass (c.m.) energies. To estimate annual event rates for specific IMH decay channels, one may multiply the production cross sections in Fig. 3 with the branching fractions from Fig. 2 and the integrated design luminosity, typically 10^4 pb^{-1} (maybe even[17] 10^5 pb^{-1}) per year. For case I [Eq. (7)] we expect several thousands of W^*W^* signal events per year, depending on M_H.

Unfortunately, IMH searches at hadron supercolliders are complicated due to large standard-model backgrounds. In this section we investigate in detail dynamical distributions of the signal

$$pp \to H \to W^*W^* \to (l\bar{\nu}_l)(\bar{l}'\nu_{l'}) \quad (l,l'=e,\mu) , \tag{14}$$

and various other processes which mimic the same final state. We show how suitable cuts on certain variables help to discriminate the signal from the backgrounds. The matrix elements of the subprocesses contributing to the signal and backgrounds were evaluated at the parton level. The cross sections and distributions were then calculated by Monte Carlo techniques and were convoluted with the set-I parton structure functions in Ref. 23 evaluated at scale $Q^2=\hat{s}$, the square of the c.m. energy of the relevant subprocess.

We consider the backgrounds

(a) $pp \to Z^*, \gamma^* \to l\bar{l}$,

(b) $pp \to Z^*, \gamma^* \to \tau\bar{\tau} \to (l\bar{\nu}_l\nu_\tau)(\bar{l}'\nu_{l'}\bar{\nu}_\tau)$,

(c_1) $pp \to ZZ \to (l\bar{l})(\nu_{l'}\bar{\nu}_{l'})$,

(c_2) $pp \to \gamma^*Z \to (l\bar{l})(\nu_{l'}\bar{\nu}_{l'})$,

(d) $pp \to t\bar{t} \to (bW^+)(\bar{b}W^-)$, with $W^+ \to \bar{l}'\nu_{l'}$ and $W^- \to l\bar{\nu}_l$

(e) $pp \to WW \to (l\bar{\nu}_l)(\bar{l}'\nu_{l'})$.

We now discuss each of these processes.

Background (a) is the Drell-Yan production of lepton pairs (electrons or muons). As this is not accompanied by missing energy, this background is easily eliminated by imposing a cut on the minimum value of the missing transverse momentum $\not{p}_T$. Because of the minimum bias hadrons, it is difficult to determine $\not{p}_T$ accurately at pp supercolliders; we therefore impose a relatively high cut, viz.,

$$\not{p}_T > 50 \text{ GeV} . \tag{15}$$

Background (b), the production of a τ lepton pair decaying leptonically, gives a $l\bar{l}'$ ($l,l'=e,\mu$) final state plus missing energy carried away by four neutrinos. The τ leptons are preferably produced near the Z-boson pole ($Z^* \to \tau\bar{\tau}$) and the photon pole ($\gamma^* \to \tau\bar{\tau}$). The τ leptons produced near the Z-boson pole are highly relativistic, and thus their decay products follow the τ direction, so that the final-state leptons are nearly back to back in the transverse plane, whereas τ leptons produced near the photon pole have low invariant mass and yield low energetic final-state leptons. We impose a cut on the maximum value of the angle in the transverse plane between the final-state leptons $\phi(l\bar{l}')$ to eliminate the $\tau\bar{\tau}$ background from Z decay. Following Ref. 24, we choose

$$\phi(l\bar{l}') < 160^\circ . \tag{16}$$

The photon-induced background may be eliminated by imposing a cut on the minimum transverse momentum of the final-state leptons, p_T. A cut

$$p_T(l), p_T(\bar{l}') > 20 \text{ GeV} \tag{17}$$

is sufficient for this purpose, provided that leptons can be measured down to this transverse momenta at the SSC and LHC.

Background (c_1) represents the continuum production of almost real Z-boson pairs, one of which decays into neutrinos and the other into electrons or muons. As the invariant mass of the electrons or muons peaks at M_Z, this background may be eliminated by imposing

$$m(l\bar{l}) < 80 \text{ GeV} , \tag{18}$$

where $m(l\bar{l})$ denotes the invariant mass of the charged-lepton pair.

Background (c_2) is the continuum production of a virtual photon and an almost real Z boson, the former decaying into charged leptons and the latter into neutrinos. Unlike the signal, this background obviously peaks at small $m(l\bar{l})$. Equivalently to rejecting small $m(l\bar{l})$ events, we impose the cut

$$\phi(l\bar{l}) > 10^\circ \tag{19}$$

to eliminate this background. The interference contribution between (c_1) and (c_2) is negligible after imposing cuts, and we do not consider it.

Since[9] $m_t > M_W$, it has become imperative to include the new background (d). We implement this by taking into account the lowest-order QCD calculations[25] for the subprocesses $gg, q\bar{q} \to t\bar{t}$ multiplied by an approximate[26] K factor 1.5 to include the next-order QCD correction. Note that there are additional particles in the final state

(viz., hadron jets originating from $b\bar{b}$); this may be used as a discriminating criterion, keeping in mind, however, that the background events containing soft hadron jets will be indistinguishable from the minimum-bias events at SSC and LHC. The characteristics of these minimum-bias events are not yet completely understood, but there seems to be general consensus that it may be difficult to identify hadron jets with $p_T \lesssim 30$ GeV. We thus require

$$p_T(b), p_T(\bar{b}) < 30 \text{ GeV} . \tag{20}$$

For a fixed center-of-mass energy, the cross section for top-quark pair production increases rapidly with decreasing m_t. At SSC energies the total cross section (without cuts) for $m_t = 125$ GeV is almost 7 times as large as that for $m_t = 200$ GeV. This process proceeds mainly through gluon fusion, and the production cross section decreases with the gluon luminosity for decreasing $\sqrt{s}$.

For a heavy top quark ($m_t \gtrsim 175$ GeV) the transverse-momentum distribution of the bottom quark into which it decays is relatively flat; however, for a lighter top quark it is sharply peaked at small $p_T(b)$. Hence the cut of Eq. (20) reduces the background with respect to the signal only for large m_t. A different strategy must be adopted for $m_t < 175$ GeV. We consider the separation between the hadron jet fragmenting from b or $\bar{b}$ and any charged lepton l or $\bar{l}'$ defined by

$$\Delta R = (\Delta\phi^2 + \Delta\eta^2)^{1/2} , \tag{21}$$

where $\Delta\phi$ is the angle between charged lepton and quark jet in the transverse plane and $\Delta\eta$ the difference in their pseudorapidities. In the IMH signal the leptons are quite isolated from the minimum-bias hadrons; however, for the $t\bar{t}$ background the distribution in $\Delta R_{\min}$, the minimum of the four possible ΔR's between the $b,\bar{b}$ and $l,\bar{l}'$ peaks at small values of $\Delta R_{\min}$. Imposing a cut on the minimum value of $\Delta R_{\min}$ improves the signal-to-background ratio considerably for the light top quark. We require $\Delta R_{\min} > 0.7$ at the parton level. One should bear in mind, however, that both the signal and background are produced by QCD processes and so will contain multiple jets from the radiation of extra gluons. Consequently, a more detailed study including hadronization will eventually be necessary to substantiate our parton-level results.

The background process of $b\bar{b}, c\bar{c}$ pair production followed by the semileptonic decay of each quark also has the same final state as the W^*W^* signal. However, the decay products of the light quarks continue moving collinearly so that the leptons and hadrons are not well isolated, and thus this background is easily distinguishable from the signal.

Background (e), which is the continuum pair production of W bosons followed by their semileptonic decay, is the largest background for our signal. We take into account the correlation between final-state leptons in this background calculation.[24] We account for virtual- and soft-gluon corrections by multiplying the lowest-order cross section for $q\bar{q} \to WW$ by the K factor[27]

$$K = 1 + \frac{8\pi}{9}\alpha_s(\hat{s}) . \tag{22}$$

This is an irreducible background for our signal—it is difficult to suppress this background by imposing cuts without also reducing the signal.

It is not possible to directly reconstruct the mass of the IMH from the final decay products for the signal under consideration due to missing energy associated with the two neutrinos. An estimate for M_H can, however, be obtained by considering the cluster transverse mass[28] defined by

$$M_T(l\bar{l}', \not{p}_T) = [\{[\mathbf{p}_T^2(l\bar{l}') + m^2(l\bar{l}')]^{1/2} + |\not{\mathbf{p}}_T|\}^2 - |\mathbf{p}_T(l\bar{l}') + \not{\mathbf{p}}_T|^2]^{1/2} , \tag{23}$$

where $\mathbf{p}_T(l\bar{l}') = \mathbf{p}_T(l) + \mathbf{p}_T(\bar{l}')$ and $\not{\mathbf{p}}_T = \mathbf{p}_T(\nu_{l'}) + \mathbf{p}_T(\bar{\nu}_l)$. The distribution in $M_T(l\bar{l}', \not{p}_T)$ for the considered signal has a broad Jacobian peak with an end point at M_H, which furnishes an estimate of the Higgs-boson mass. In a similar way we can define M_T for both the $t\bar{t}$ and continuum WW backgrounds.

In order to reduce the continuum WW background, we impose additional cuts on the maximum values of the variables $p_T(l)$, $p_T(\bar{l}')$, $\not{p}_T$, $m(l\bar{l}')$, and $M_T(l\bar{l}', \not{p}_T)$. The cuts are chosen such that they exclude events beyond the end points of the distributions for the largest M_H value considered in the signal, viz., $M_H = 180$ GeV; this effectively reduces the backgrounds without any reduction in the IMH signal rate. We summarize below all the cuts that we impose on both the signal and backgrounds:

TABLE I. $H \to W^*W^* \to (l\bar{\nu}_l)(\bar{l}'\nu_{l'})$ signal and background cross sections (in femtobarns) integrated over $m(l\bar{l}')$ up to $m(l\bar{l}')_{\max}$ for $m_t = 200$ GeV at the SSC, $\sqrt{s} = 40$ TeV. The results are summed over $l, l' = e, \mu$, and the cuts in Eqs. (24) and (25) are imposed.

Signal M_H (GeV) \ $m(l\bar{l}')_{\max}$ (GeV)	80.0	60.0	50.0	40.0	30.0	20.0
180	668	508	403	282	162	66.3
160	759	703	607	462	286	122
150	405	377	326	257	161	81.3
145	279	264	230	186	123	48.3
140	185	179	162	132	90.8	36.2
$t\bar{t}$ background			negligible			
WW background	604	411	333	209	135	48.4

TABLE II. $H \to W^* W^* \to (l\bar{\nu}_l)(\bar{l}'\nu_{l'})$ signal and background cross sections (in femtobarns) integrated over $m(l\bar{l}')$ up to $m(l\bar{l}')_{\max}$ for $m_t = 150$ GeV at the SSC, $\sqrt{s} = 40$ TeV. The results are summed over $l, l' = e, \mu$, and the cuts in Eqs. (24) and (25) are imposed.

Signal M_H (GeV) \ $m(l\bar{l}')_{\max}$ (GeV)	80.0	60.0	50.0	40.0	30.0	20.0
180	733	558	442	309	176	72.7
160	815	754	651	496	307	131
150	430	400	347	273	171	86.3
145	295	280	243	196	130	51.1
140	194	188	170	139	95.6	38.1
$t\bar{t}$ background	790	446	326	191	123	36.2
WW background	604	411	333	209	135	48.4
Sum of the two backgrounds	1394	857	659	400	258	84.6

(i) $20\ \text{GeV} < p_T(l) < 100\ \text{GeV}$,

(ii) $|y(l)| < 3$,

(iii) $50\ \text{GeV} < \not{p}_T < 100\ \text{GeV}$,

(iv) $m(l\bar{l}') < 80\ \text{GeV}$, (24)

(v) $M_T(l\bar{l}', \not{p}_T) < 200\ \text{GeV}$,

(vi) $10^\circ < \phi(l\bar{l}') < 160^\circ$.

In addition, to further reduce the $t\bar{t}$ background, we impose the cuts

(vii) $p_T(b),\ p_T(\bar{b}) < 30\ \text{GeV},\ \Delta R_{\min} > 0.7$. (25)

We investigate in detail the cases for top-quark-mass values of 150 and 200 GeV at SSC ($\sqrt{s} = 40$ TeV) and LHC ($\sqrt{s} = 16$ TeV) energies. For $m_t = 200$ GeV the $t\bar{t}$ background after cuts is negligible compared to either the signal or the continuum WW background at both SSC and LHC. However, for $m_t = 150$ GeV the $t\bar{t}$ background is comparable to the signal and WW background. For this case we add the two backgrounds (since they have the same final-state modulo soft b hadron jets) to obtain the total background to our signal. We find that for $m_t = 200$ GeV the signal is easily discriminated from the backgrounds. However, the separation of signal and background becomes problematic at lower m_t, and below $m_t = 150$ GeV the signal ceases to be observable. In Figs. 4(a)–4(c) we present the distributions in the variables $m(l\bar{l}')$, $p_T(l)$, and $M_T(l\bar{l}', \not{p}_T)$ for the signal and backgrounds for $m_t = 200$ GeV at the SSC. The dilepton invariant mass turns out to be the most effective variable for discriminating the signal from the backgrounds.

The $m(l\bar{l}')$ distribution of the signal cuts off rapidly above $m(l\bar{l}') > M_H/3$, whereas the backgrounds extend out to higher $m(l\bar{l}')$. Thus it is advantageous to impose a cut on a maximum $m(l\bar{l}')$. In Tables I–IV we present the cross sections for the signal and backgrounds integrated over $m(l\bar{l}')$ up to $m(l\bar{l}')_{\max} = 20$, 30, 40, 50, 60, and 80 GeV.

For the case $m_t = 200$ GeV we see from Table I and Fig. 4(a) that the ratio of the signal to the WW background is about 1 for $M_H = 145$ GeV and $m(l\bar{l}')_{\max} = 20$ GeV. The total signal cross section in this case is 48 fb, which corresponds to 480 events per year at the SSC design luminosity of 10 fb^{-1}/yr. For $M_H \gtrsim 150$ GeV the signal is observable for $m(l\bar{l}') < 50$ GeV. Thus, if $m_t \approx 200$ GeV, we conclude that the IMH can be observed at the SSC for $M_H > 145$ GeV.

For $m_t = 150$ GeV it can be seen from Table II and Fig.

TABLE III. $H \to W^* W^* \to (l\bar{\nu}_l)(\bar{l}'\nu_{l'})$ signal and background cross sections (in femtobarns) integrated over $m(l\bar{l}')$ up to $m(l\bar{l}')_{\max}$ for $m_t = 200$ GeV at the LHC, $\sqrt{s} = 16$ TeV. The results are summed over $l, l' = e, \mu$, and the cuts in Eqs. (24) and (25) are imposed.

Signal M_H (GeV) \ $m(l\bar{l}')_{\max}$ (GeV)	80.0	60.0	50.0	40.0	30.0	20.0
180	189	143	113	78.8	46.0	18.8
160	225	208	179	134	82.0	33.9
150	119	110	94.9	73.0	44.4	19.2
140	56.9	55.1	49.7	40.4	27.8	11.2
$t\bar{t}$ background			negligible			
WW background	292	200	161	101	65.9	23.4

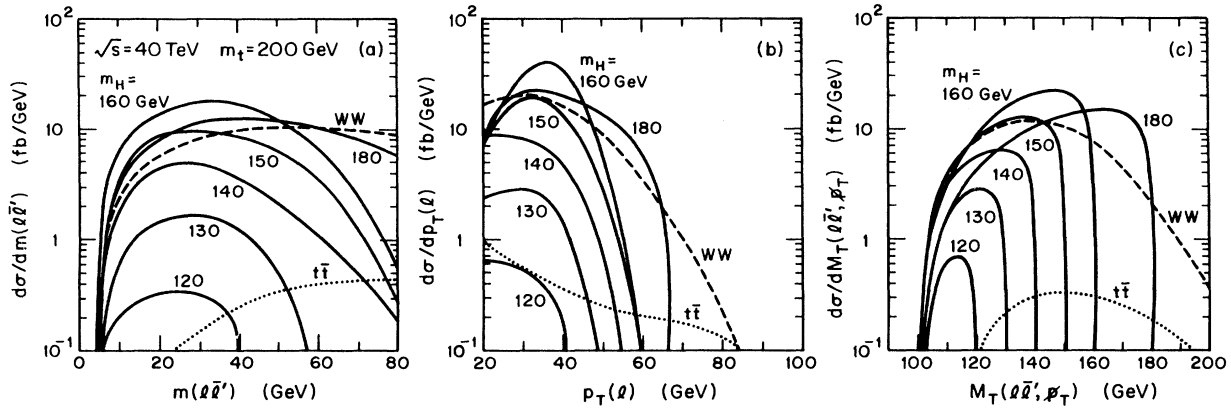

FIG. 4. Distributions in (a) $m(l\bar{l}')$, the invariant mass of the charged dileptons, (b) $p_T(l)$, the transverse momentum of the charged lepton, and (c) $M_T(l\bar{l}', \not{p}_T)$, the cluster transverse mass of the charged dileptons and neutrinos, for the $H \to W^*W^* \to (l\bar{\nu}_l)(\bar{l}'\nu_{l'})$ $(l,l'=e,\mu)$ signal and the continuum WW and $t\bar{t}$ backgrounds at $\sqrt{s}=40$ TeV and $m_t=200$ GeV.

5(a) that the signal-to-total-background ratio at the SSC is about 1 for $M_H=150$ GeV with a maximum invariant dilepton mass of 20 GeV. Then we expect a total of 860 signal events per year. We conclude that the $H \to W^*W^*$ signal at the SSC should be observable for IMH masses between 150 and 160 GeV when $m_t=150$ GeV in events with $m(l\bar{l}')<20$ GeV.

At LHC the total cross sections for both signal and $t\bar{t}$ background are smaller by a factor of 3–4, since both depend on the gluon luminosity. However, the continuum WW background which depends on quark-antiquark luminosities decreases only by a factor of about 2. Thus the prospects of observing the IMH at the LHC are worse than those at the SSC.

For $m_t=200$ GeV the Higgs-boson signal at the LHC is observable over the WW background for $M_H \gtrsim 150$ GeV in events with an invariant dilepton mass of less than 20 GeV. As can be seen from Fig. 6 and Table III, the signal is exceptionally promising for an IMH mass close to the threshold for Higgs-boson decay into two real W bosons; for $M_H=160$ GeV the annual event rate is 1340 imposing $m(l\bar{l}')<40$ GeV and assuming an integrated luminosity of 10 fb^{-1}.

For $m_t=150$ GeV the prospects for finding the IMH at the LHC are not so promising (see Fig. 7 and Table IV). Only for $M_H \approx 2M_W$ does the signal exceed the total background for $m(l\bar{l}')<30$ GeV. At threshold the annual signal event rate is 360. For $m_t \gtrsim 200$ GeV the $t\bar{t}$ background is much smaller than the IMH signal, and so detection of the signal at both SSC and LHC is limited only by the continuum WW background.

We conclude that a measurement of events with small

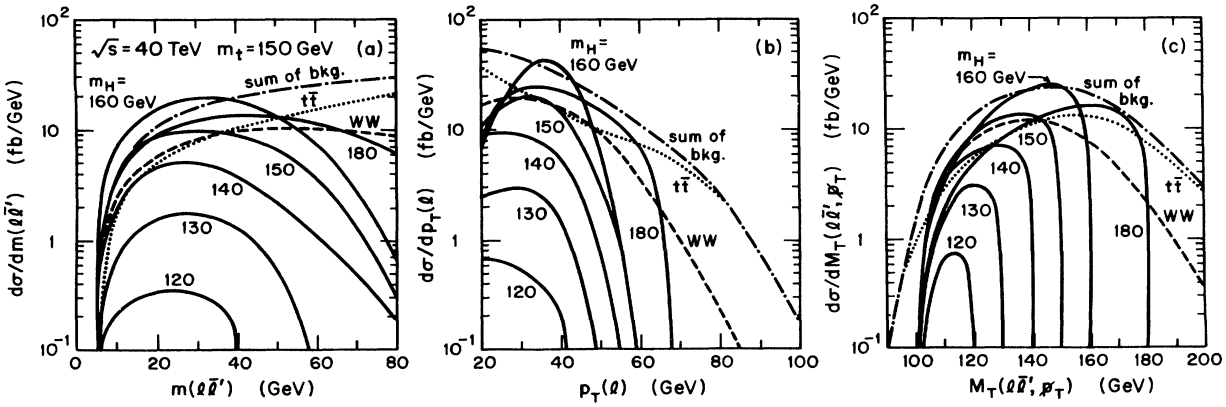

FIG. 5. Distributions in (a) $m(l\bar{l}')$, the invariant mass of charged dileptons, (b) $p_T(l)$, the transverse momentum of the charged lepton, and (c) $M_T(l\bar{l}', \not{p}_T)$, the cluster transverse mass of the charged dileptons and neutrinos, for the $H \to W^*W^* \to (l\bar{\nu}_l)(\bar{l}'\nu_{l'})$ $(l,l'=e,\mu)$ signal, the continuum WW background, the $t\bar{t}$ background, and the sum of the two backgrounds at $\sqrt{s}=40$ TeV and $m_t=150$ GeV.

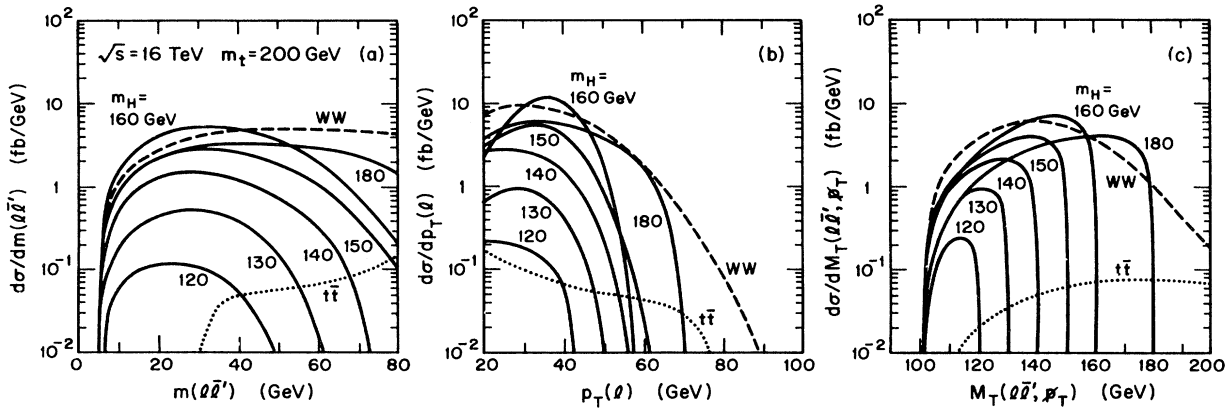

FIG. 6. Distributions in (a) $m(l\bar{l}')$, the invariant mass of charged dileptons, (b) $p_T(l)$, the transverse momentum of the charged lepton, and (c) $M_T(l\bar{l}',\not{p}_T)$, the cluster transverse mass of the charged dileptons and neutrinos, for the $H\to W^*W^*\to(l\bar{\nu}_l)(\bar{l}'\nu_{l'})$ $(l,l'=e,\mu)$ signal and the continuum WW and $t\bar{t}$ backgrounds at $\sqrt{s}=16$ TeV and $m_t=200$ GeV.

invariant dilepton mass $[m(l\bar{l}')\lesssim 30$ GeV] is crucial for the discovery of the IMH at future hadron supercolliders. Once the IMH is seen as an enhancement over SM backgrounds at low values of $m(l\bar{l}')$, its mass can be indirectly measured from the end point of the M_T distribution. We also note that the $p_T(l)$ distribution for the signal, especially near the WW pair threshold, is sharply peaked over the total background for $p_T(l)<50$ GeV (except for the case $m_t=150$ GeV at LHC) and thus provides an additional means for the discovery of the IMH.

There are other potential backgrounds not addressed above, such as $b\bar{b}b\bar{b}$ and $Wb\bar{b}$ with two charged leptons from $b,\bar{b}$, or W decays. In fact, these processes have larger cross sections than the IMH signal. However, in these events the leptons from b decays are rather soft and there will be more hadron or jet activity. Therefore, the cuts in Eqs. (24) and (25) along with lepton isolation considerations should be effective in eliminating these backgrounds.

IV. SUMMARY

We have calculated the branching fractions of $H\to W^*W^*$ and Z^*Z^* for the intermediate-mass Higgs boson taking into account the QCD corrections to ha-

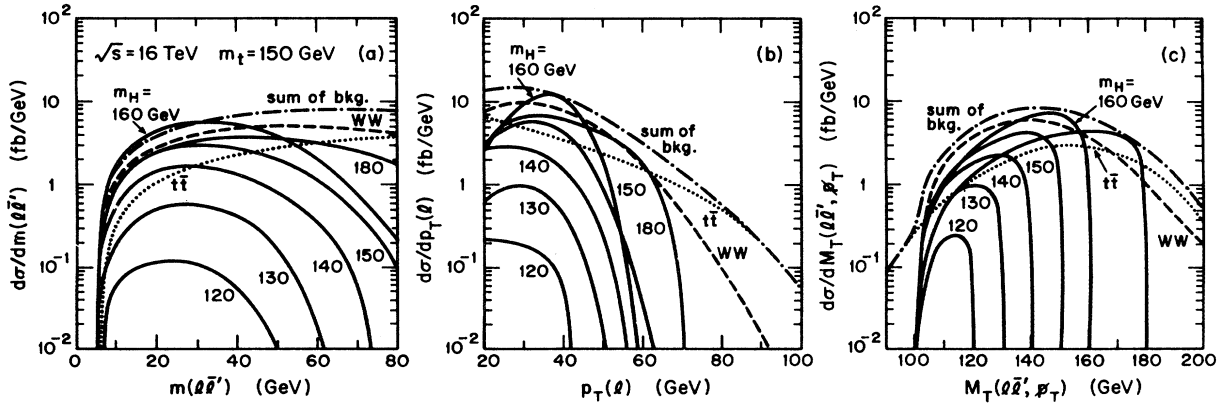

FIG. 7. Distributions in (a) $m(l\bar{l}')$, the invariant mass of charged dileptons, (b) $p_T(l)$, the transverse momentum of the charged lepton, and (c) $M_T(l\bar{l}',\not{p}_T)$, the cluster transverse mass of the charged dileptons and neutrinos, for the $H\to W^*W^*\to(l\bar{\nu}_l)(\bar{l}'\nu_{l'})$ $(l,l'=e,\mu)$ signal, the continuum WW background, the $t\bar{t}$ background, and the sum of the two backgrounds at $\sqrt{s}=16$ TeV and $m_t=150$ GeV.

TABLE IV. $H \to W^* W^* \to (l\bar{\nu}_l)(\bar{l}'\nu_{l'})$ signal and background cross sections (in femtobarns) integrated over $m(l\bar{l}')$ up to $m(l\bar{l}')_{\max}$ for $m_t = 150$ GeV at the LHC, $\sqrt{s} = 16$ TeV. The results are summed over $l, l' = e, \mu$, and the cuts in Eqs. (24) and (25) are imposed.

Signal M_H (GeV) \ $m(l\bar{l}')_{\max}$ (GeV)	80.0	60.0	50.0	40.0	30.0	20.0
180	208	158	124	86.5	50.5	20.6
160	241	223	192	144	88.0	36.3
150	127	117	101	77.6	47.2	20.5
140	60.0	58.0	52.4	42.5	29.3	11.8
$t\bar{t}$ background	166	93.9	71.0	40.2	25.3	7.66
WW background	292	200	161	101	65.9	23.4
Sum of the two backgrounds	458	294	232	141	91.2	31.1

dronic Higgs-boson decays. We examined in detail the IMH signal from $H \to W^* W^* \to (l\bar{\nu}_l)(\bar{l}'\nu_{l'})$ as well as the two major backgrounds: continuum W pair and $t\bar{t} \to (Wb)(\bar{W}\bar{b})$ production. The signal rate is large (several thousand events per SSC year), but the backgrounds are severe. After a set of selective cuts [Eqs. (24) and (25)], the continuum W pair background can be suppressed below the signal for $M_H \gtrsim 150$ GeV. Including the $t\bar{t}$ background, the IMH signal via $W^* W^*$ leptonic decays may be observable with signal/background $\gtrsim 1$ if $m_t \gtrsim 150$ GeV.

ACKNOWLEDGMENTS

We thank H. Baer and F. Paige for helpful discussions. One of us (B.A.K.) would like to thank Z. Kunszt for useful communications regarding the effect of running quark masses. This research was supported in part by the University of Wisconsin Research Committee with funds granted by the Wisconsin Alumni Research Foundation and in part by the U.S. Department of Energy under Contract No. DE-AC02-76ER00881.

*Present address: Fermi National Accelerator Laboratory, Batavia, IL 60510.

[1]V. Barger, in *Proceedings of the XXIV International Conference on High Energy Physics,* Munich, West Germany, 1988, edited by R. Kotthaus and J. Kühn (Springer, Berlin, 1989), p. 1265, and references therein.

[2]J. F. Gunion, H. E. Haber, G. L. Kane, and S. Dawson, *The Higgs Hunter's Guide* (Addison-Wesley, Redwood City, CA, 1990).

[3]ALEPH Collaboration, D. Decamp *et al.*, Phys. Lett. B **246**, 306 (1990).

[4]M. Veltman, Acta Phys. Pol. B **8**, 475 (1977); B. W. Lee, C. Quigg, and H. B. Thacker, Phys. Rev. Lett. **38**, 883 (1977); Phys. Rev. D **16**, 1519 (1977); M. S. Chanowitz and M. K. Gaillard, Nucl. Phys. **B261**, 379 (1985); M. S. Chanowitz, Annu. Rev. Nucl. Part. Phys. **38**, 323 (1988).

[5]J. D. Bjorken, SLAC Report No. 198, 1976 (unpublished).

[6]S. L. Wu *et al.*, ECFA workshop, Report No. CERN-EP/87-40 (unpublished); M. Drees *et al.*, in *Z Physics at LEP I,* proceedings of the Workshop, Geneva, Switzerland, 1989, edited by G. Altarelli, R. Kleiss, and C. Verzegnassi (CERN Yellow Report No. 89-08, Geneva, 1989), Vol. 2, p. 59.

[7]R. N. Cahn and S. Dawson, Phys. Lett. **136B**, 196 (1984); G. Kane, W. Repko, and W. Rolnick, *ibid.* **148B**, 367 (1984); S. Dawson, Nucl. Phys. **B249**, 42 (1985); G. Altarelli, B. Mele, and F. Pitolli, Nucl. Phys. **B287**, 205 (1987); A. Tofighi-Niaki and J. Gunion, Phys. Rev. D **36**, 2671 (1987); **38**, 1433 (1988).

[8]J. F. Gunion, G. L. Kane, and J. Wudka, Nucl. Phys. **B299**, 231 (1988).

[9]CDF Collaboration, H. B. Jensen, Bull. Am. Phys. Soc. **35**, 943 (1990).

[10]E. Braaten and J. P. Leveille, Phys. Rev. D **22**, 715 (1980); M. Drees and K.-I. Hikasa, Phys. Lett. B **240**, 455 (1990).

[11]J. F. Gunion, P. Kalyniak, M. Soldate, and P. Galison, Phys. Rev. D **34**, 101 (1986).

[12]A. Seiden, *High Energy Physics in the 1990's (Snowmass 1988),* proceedings of the Summer Study, Snowmass, Colorado, 1988, edited by S. Jensen (World Scientific, Singapore, 1989).

[13]G. Kane, talk presented at the 1990 Summer Study on High Energy Physics, Snowmass, Colorado, 1990 (unpublished).

[14]T. G. Rizzo, Phys. Rev. D **22**, 722 (1980); W.-Y. Keung and W. Marciano, *ibid.* **30**, 248 (1984).

[15]J. F. Gunion, Z. Kunszt, and M. Soldate, Phys. Lett. **163B**, 389 (1985); **168B**, 427(E) (1986); W. J. Stirling, R. Kleiss, and S. D. Ellis, *ibid.* **163B**, 261 (1985).

[16]E. W. N. Glover, J. Ohnemus, and S. S. D. Willenbrock, Phys. Rev. D **37**, 3193 (1988).

[17]F. Paige, talk presented at the 1990 Summer Study on High Energy Physics, Snowmass, Colorado, 1990 (unpublished).

[18]M_W is measured at hadron colliders: CDF Collaboration, P. Schlabach, Bull Am. Phys. Soc. **35**, 999 (1990); UA2 Collaboration, S. Lami, presented at the Z Phenomenology Symposium, Madison, Wisconsin, 1990 (unpublished). The M_Z value used here is a weighted average of the results presented in talks by H. Zobernig (ALEPH Collaboration), A. Firestone (DELPHI Collaboration), F. Linde (L3 Collaboration), and R. Barlow (OPAL Collaboration) at the Z Phenomenology Symposium, Madison, Wisconsin, 1990 (unpublished).

[19]W. J. Marciano, Phys. Rev. D **29**, 580 (1984).

[20]A. Barroso, J. Pulido, and J. C. Romão, Nucl. Phys. **B267**, 509 (1986).

[21]B. A. Kniehl, Phys. Lett. B **244**, 537 (1990).

[22]H. M. Georgi, S. L. Glashow, M. E. Machacek, and D. V.

Nanopoulos, Phys. Rev. Lett. **40**, 692 (1978).
[23]E. Eichten, I. Hinchliffe, K. Lane, and C. Quigg, Rev. Mod. Phys. **56**, 579 (1984); **58**, 1065(E) (1986).
[24]V. Barger, T. Han, and J. Ohnemus, Phys. Rev. D **37**, 1174 (1988).
[25]B. L. Combridge, Nucl. Phys. **B151**, 429 (1979).
[26]P. Nason, S. Dawson, and R. K. Ellis, Nucl. Phys. **B303**, 607 (1988); H. Baer, V. Barger, H. Goldberg, and J. Ohnemus, Phys. Rev. D **38**, 3467 (1988).
[27]V. Barger, J. L. Lopez, and W. Puttika, Int. J. Mod. Phys. A **3**, 2181 (1988).
[28]V. Barger, A. D. Martin, and R. J. N. Phillips, Z. Phys. C **21**, 99 (1983).